Ecological Modelling 425 (2020) 109033

Contents lists available at ScienceDirect

Ecological Modelling

journal homepage: www.elsevier.com/locate/ecolmodel

An approach to modeling resource optimization for substitutable and interdependent resources

Edward B. Rastetter*, Bonnie L. Kwiatkowski

The Ecosystems Center, Marine Biological Laboratory, Woods Hole, MA 02543, USA

ARTICLE INFO

Keywords:
Resource optimization
Acclimation
Substitutable resources
Interdependent resources
Resource limitation
Multiple resource limitation

ABSTRACT

We develop a hierarchical approach to modeling organism acclimation to changing availability of and requirements for substitutable and interdependent resources. Substitutable resources are resources that fill the same metabolic or stoichiometric need of the organism. Interdependent resources are resources whose acquisition or expenditure are tightly linked (e.g., light, CO_2, and water in photosynthesis and associated transpiration). We illustrate the approach by simulating the development of vegetation with four substitutable sources of N that differ only in the cost of their uptake and assimilation. As the vegetation develops, it uses the least expensive N source first then uses progressively more expensive N sources as the less expensive sources are depleted. Transition among N sources is based on the marginal yield of N per unit effort expended, including effort expended to acquire C to cover the progressively higher uptake costs. We illustrate the approach to interdependent resources by simulating the expenditure of effort to acquire light energy, CO_2, and water to drive photosynthesis in vegetation acclimated to different conditions of soil water, atmospheric vapor pressure deficit, CO_2 concentration, and light levels. The approach is an improvement on the resource optimization used in the earlier Multiple Element Limitation (MEL) model.

1. Introduction

Evolution has given rise to species with remarkable abilities to survive in environments where the supply of resources differs significantly from the requirements of the organisms themselves (Shaver and Melillo 1984, Ågren and Bosatta 1996). In such environments, the struggle for existence should favor organisms able to optimize the expenditure of their internal assets (e.g., tissue distribution, enzyme production, energy use) to acquire resources from the environment (e.g., carbon [C], nitrogen [N], water, energy) in proportion to their metabolic and stoichiometric needs (Chapin et al. 1987). Although the mechanisms of optimization vary among species, a general theory of optimal resource acquisition has gradually emerged in the literature over the past fifty years. These contributions include syntheses on biomass allocation in plants (Mooney 1972), optimization of plant function in response to CO_2, temperature, light, and nutrients (Field et al. 1992), cost-benefit analysis of taking up various forms of N (Gutschick 1981), optimization of resource acquisition to maintain metabolic and stoichiometric balance using an economic analogy (Bloom et al. 1985, Chapin et al. 1987), and theoretical assessments of source-sink controls on resource acquisition, production, and allometry (Hilbert 1990, Ågren and Bosatta 1996, Farrar and Jones 2000, Kröner 2015). Several models have been built based on optimization of resource acquisition as an improvement on Leibig's Law or concurrent limitation approaches (Rastetter 2011). For example, Thronley's (1972) model adjusts root versus shoot growth based on colimitation of both tissues by C and nutrients, source-sink dynamics between roots and shoots, and the counterflow of C versus nutrients between the two tissues. Olson et al. (1985) use a continuous-time Markov approach to simulate transitions among various plant states, with each state responsible for uptake of a different resource. Vallino et al. (1996) use a linear programing approach to maximize growth in relation to the acquisition of alternative resources and their processing through various metabolic pathways. Rastetter and Shaver (1992) and Rastetter et al. (1997) examine limitation using a model that optimizes allocation of uptake effort to maintain stoichiometric balance based on the resource optimization paradigm that underlies this body of literature. In this paper we build on the approach used by Rastetter and Shaver (1992) to simulate resource optimization for two specific classes of resource: substitutable resources and interdependent resources.

Substitutable resources are resources that fulfill the same stoichiometric and metabolic requirements of the organism (Tilman 1982). For example, the N requirements of a plant can be met through the uptake of NH_4^+ or NO_3^-, mycorrhizal acquisition of organic N, and symbiotic N fixation. From the plant's perspective, these N sources differ

* Corresponding author.
E-mail addresses: erastetter@mbl.edu (E.B. Rastetter), bkwiatkowski@mbl.edu (B.L. Kwiatkowski).

https://doi.org/10.1016/j.ecolmodel.2020.109033
Received 4 November 2019; Received in revised form 9 March 2020; Accepted 10 March 2020
Available online 31 March 2020

significantly in their acquisition and assimilation cost. This difference in cost arises largely because of the need to build and maintain tissues to reach and take up these N sources, to supply carbohydrate to the symbionts, or to expend energy, for example, to reduce NO_3^-. The return on this expenditure decreases as the availability of the resource in the environment declines, making the overall cost per unit resource assimilated rise. Because of this rise in the unit cost, it can become advantageous for the organism to shift asset expenditure toward another substitutable resource with a lower overall cost per unit resource return. For example, as NH_4^+ is depleted more assets must be expended to maintain its rate of uptake, thereby increasing the cost per unit N taken up. It might therefore be more efficient to shift from NH_4^+ to NO_3^- uptake despite the extra cost of reducing the N in NO_3^-.

Acquisition of *interdependent resources* are closely linked to one another such that they must be taken up concurrently. For example, in vascular plants, photosynthesis requires the acquisition of light energy, CO_2, and water to produce carbohydrate and replace water lost in transpiration. Clearly, at a molecular scale the acquisition of these resources can be treated as separate (Farquhar 1989), but at a plant or vegetation scale these processes are often treated as interdependent (Parton et al. 1993, Ryan et al. 1996, Rastetter et al. 2013). In either case, to maximize carbohydrate production per uptake asset expended requires an optimal distribution of those uptake assets among light, CO_2, and water acquisition.

We develop equations to simulate optimization of substitutable and interdependent resource acquisition. The approach is essentially the same for both types of resource. We define an abstract quantity we call "effort" that represents all plant assets available to acquire resources from the environment. We then redistribute this effort hierarchically:

1st: Redistribute effort toward element resources in short supply and away from element resources in surfeit to better meet stoichiometric and metabolic requirements.

2nd: Redistribute effort allocated to each element resource among substitutable or interdependent resources to increase element return per unit effort expended.

The only difference between our approaches to substitutable and interdependent resources is in the assessment of effort expended to cover secondary costs of assimilation (e.g., energy cost of reducing NO_3^- or carbohydrate cost of supporting symbionts). Each substitutable resource will have an independent secondary cost of assimilation that needs to be factored into the assessment of element return per unit effort. Secondary costs cannot be separated for interdependent resources and hence the secondary costs are shared equally among interdependent resources.

We draw a distinction between *optimized* and *optimizing*. There are many approaches for calculating or searching for optimal solutions to equations (e.g., Press et al. 1986). The result of those approaches is an optimized solution within specified constraints. The equations we present below do not yield optimized solutions except asymptotically over time as the simulated organisms adapt to a constant environment. Instead, the equations we present mimic the incremental redistribution of uptake assets within an organism that drive that distribution toward an optimum, but do not necessarily find that optimum before the environment, and therefore the optimum, changes. The equations are in this sense optimizing, but the distribution of uptake assets is not necessarily optimized.

Motivation for this work is twofold. First, we are interested in exploring the nature of limitation by substitutable and interdependent resources in the context of a simple heuristic model. The second motivation is more pragmatic; we want to document a solution to dealing with substitutable and interdependent resources we encountered in an earlier version of the Multiple Element Limitation (MEL) model (Rastetter et al. 2013).

In that earlier model, a single equation was used to calculate allocation of uptake effort among elements as well as substitutable sources of those elements. This approach made the calculations unnecessarily complex and difficult to apply because the criteria for allocation differ; allocation among elements is driven by stoichiometry whereas allocation among substitutable resources is driven by the return per incremental increase in effort expended (i.e., marginal yield). In the earlier model, we allocated effort by first calculating the requirements for each element resource based on element turnover in biomass. We then partitioned those requirements among substitutable resources with the partitioning strongly favoring substitutable resources with a high marginal yield. Finally, we redistributed uptake effort toward a condition where the ratio of requirement to uptake is the same for all resources (Bloom et al. 1985), including substitutable resources. This approach caused two problems. First, finding the balance of allocation among substitutable sources of one element was confounded by their interactions with all the other elements, making the model more difficult to implement. Second, because the allocation was based on the ratio of requirement to uptake, there were numerical problems when both requirement and uptake approached zero; under such conditions even very small changes in either requirement or uptake can cause large changes in their ratio. Interdependent resources were less problematic because their requirement rarely approaches zero. However, the confounding interactions between interdependent and the other resources was still problematic.

To overcome these issues, we now calculate allocation of uptake effort hierarchically. We first allocate primary uptake effort among the elements using essentially the same strategy used in the earlier model. We then partitioning this primary effort among sub-efforts targeted toward the acquisition of substitutable or interdependent resources. Allocation of these sub-efforts is based solely on their relative marginal yields; the ratio of requirement to uptake is no longer part of this calculation. In addition, the hierarchical approach segregates each group of substitutable or interdependent resources from the other resources and thereby alleviates the problem of confounding interactions. Details of this new allocation algorithm are described below in the section on "Allocation of uptake effort."

2. Methods

We build two models based on mass-balance differential equations (Tables 1 and 2). The differential equations are solved numerically with a 4th/5th order Runge-Kutta integrator with adapting time steps to optimize precision and computation time (Press et al. 1986). The models are coded in Lazarus 2.0.4 (2019) Free Pascal. Input to the models are all parameter values, initial values for all state variables, and values for all driver variables for all time steps (in the "description" columns of Tables 1 and 2, parameters, state variables, process variables and driver variables are distinguished, respectively, by (p), (S), (P), and (D)). Outputs from the models are all state and process variables for each time step.

2.1. Model I: substitutable resources

We deliberately use a very simple model structure to amplify the heuristic value of the analysis (Rastetter 2017). As a framework from which to illustrate resource optimization for substitutable resources, we build a mass-balance model for C and N in the biomass of an idealized vegetation (B_i) based on uptake (U_i), turnover (T_i), and respiration (R_C; Table 1 Eqs. 1.1 & 1.2). We simulate the concentrations in the environment of various N sources (N_k) based on a simple mass balance of inputs to the environment (I_k) minus uptake by the vegetation (U_k) minus losses from the environment (L_k; Eq. 1.3).

As with the Multiple Element Limitation (MEL) model (Rastetter and Shaver 1992, Rastetter et al. 2013, Pearce et al. 2015, Jiang et al. 2017), asset allocation toward resource acquisition is represented by an abstract quantity we call "effort". Unlike past versions of the MEL model, here we distribute effort hierarchically; first the primary effort is allocated toward acquiring C versus N (V_i; Eq. 1.4), then the primary effort allocated toward

Table 1
Model I equations for substitutable resources. Variable and parameter values and definitions below equations.

1.1	$\frac{dB_C}{dt} = U_C - T_C - R_C$	1.2	$\frac{dB_N}{dt} = U_N - T_N$		
1.3	$\frac{dN_k}{dt} = I_k - U_k - L_k$	1.4	$\frac{dV_i}{dt} = a\ \ln(\ \Phi\frac{\Psi_i}{\bar{U}_i})\ V_i$		
1.5	$\frac{dv_{Nk}}{dt} = \omega g(\frac{y_{Nk}}{y_{max}} - \beta) max(v_{Nk},\ \varepsilon_k)$	1.6	$\frac{d\bar{\Psi}_i}{dt} = \rho(\Psi_i - \bar{\Psi}_i)$		
1.7	$\frac{d\bar{U}_i}{dt} = \rho(U_i - \bar{U}_i)$	1.8	$U_C = \frac{P_{max}}{k_I}\ \ln\{\frac{\eta\ +\ I}{\eta\ +\ I\ e^{-k_I\ L_{AI}}}\}$		
1.9	$U_N = \sum_k U_k$	1.10	$U_k = S\ \frac{g_k\ N_k}{k_k + N_k}\ V_N v_{Nk}$		
1.11	$R_C = r_C\ \Theta\ B_C + \sum_k (\phi_k U_k)$	1.12	$T_C = m_C\ \ B_C$		
1.13	$T_N = \frac{m_N\ B_N}{\Theta}$	1.14	$\Phi = \prod_i (\frac{\bar{U}_i}{\Psi_i})^{V_i}$		
1.15	$\Psi_C = \frac{(r_C + m_C)\ B_C + \sum_k (\phi_{ik} U_k)}{\Theta}$	1.16	$\Psi_N = m_N\ \Theta\ B_N$		
1.17	$S = B_C(\frac{\alpha B_C + 1}{\gamma B_C + 1})$	1.18	$\Theta = \frac{B_C}{B_N q_B}$	1.19	$L_{AI} = \lambda\ S\ V_C$
1.20	$y_{max} = max(y_{Nk})$	1.21	$\beta = \frac{\sum_k (y_{Nk} max(v_{Nk},\ \varepsilon_k))}{y_{max} \sum_k (max(v_{Nk},\ \varepsilon_k))}$		
1.22	$\varepsilon_k = \varepsilon_0$ if $y_{Nk} = y_{max}$ $\varepsilon_k = 0$ otherwise				
1.23	$L_k = \tau_k N_k$				
1.24	$y_{Nk} = \lim_{\Delta v_{Nk} \to 0} (\frac{\Delta U_N}{V_N \Delta v_{Nk} + \Delta U_N\ \phi_k (\frac{dU_C}{dV_C})^{-1}}) = \frac{\frac{dU_N}{dv_{Nk}}}{V_N + \frac{dU_N}{dv_{Nk}} \phi_k (\frac{dU_C}{dV_C})^{-1}}$				

Variables and Parameters (for i = C or N; k = 1, 2, 3, or 4). In description, (p) – parameter, (S) – state variable, (P) – process variable, (D) – driver variable

Symbol	value	units	description
a	0.002	day^{-1}	(p) effort allocation rate
B_C	Variable	g C m^{-2}	(S) vegetation C
B_N	Variable	g N m^{-2}	(S) vegetation N
g_k	0.0025	g N g^{-1}C day^{-1}	(p) N-uptake rate constant for k = 1, 2, 3, & 4
I	10	MJ m^{-2} day^{-1}	(D) irradiance
I_k	0.07	g N m^{-2} day^{-1}	(D) N inputs to source k
k_I	0.5	m^2 m^{-2}	(p) Beer's coefficient
k_k	0.1	g N m^{-2}	(p) N half saturation constant for k = 1, 2, 3, & 4
L_{AI}	Variable	m^2 m^{-2}	(P) leaf area index
L_k	Variable	g N m^{-2} day^{-1}	(P) N loss from source k
m_C	0.00025	day^{-1}	(p) C turnover coefficient
m_N	0.002	day^{-1}	(p) N turnover coefficient
N_k	Variable	g N m^{-2}	(S) available N, for k = 1, 2, 3, & 4
P_{max}	4	g C m^{-2} leaf day^{-1}	(p) maximum leaf-level photosynthesis
q_B	100	g C g^{-1} N	(p) biomass optimum C:N ratio
r_C	0.00025	day^{-1}	(p) respiration coefficient
R_C	Variable	g C m^{-2} day^{-1}	(P) respiration
S	Variable	g C m^{-2}	(P) biomass active in uptake
T_C	Variable	g C m^{-2} day^{-1}	(P) C turnover in litter
T_N	Variable	g N m^{-2} day^{-1}	(P) N turnover in litter
U_C	Variable	g C m^{-2} day^{-1}	(P) uptake of C
$\bar{U}_C$	Variable	g C m^{-2} day^{-1}	(S) integrated uptake of C
U_N	Variable	g N m^{-2} day^{-1}	(P) uptake of N
$\bar{U}_N$	Variable	g N m^{-2} day^{-1}	(S) integrated uptake of N
U_{Nk}	Variable	g N m^{-2} day^{-1}	(P) uptake of N from source k
V_C	Variable	none	(S) effort toward C
V_N	Variable	none	(S) effort toward N
v_{Nk}	Variable	none	(S) sub-effort toward N source k
y_{max}	Variable	g N m^{-2} day^{-1}	(P) maximum marginal yield of N
y_{Nk}	Variable	g N m^{-2} day^{-1}	(P) marginal yield of N from source k
α	0.000006	m^2 g^{-1}C	(p) allometric constant
β	Variable	none	(P) sub-effort balance correction
γ	0.0045	m^2 g^{-1}C	(p) allometric constant
ε_0	0.001	none	(p) sub-effort initiator constant
ε_k	Variable	fraction	(P) sub-effort initiator for k = 1, 2, 3, & 4
η	7	MJ m^{-2} day^{-1}	(p) irradiance half saturation constant
Θ	Variable	none	(P) stoichiometric constraint
λ	0.0313	m^2 g^{-1}C	(p) specific leaf area
ρ	0.002	day^{-1}	(p) uptake & requirement integration constant
τ_k	0.07	day^{-1}	(p) N-loss parameter for k = 1, 2, 3, & 4
Φ	Variable	none	(P) weighted geometric mean uptake:requirement
ϕ_1	0	g C g^{-1} N	(p) C cost of N source 1
ϕ_2	3	g C g^{-1} N	(p) C cost of N source 2
ϕ_3	6	g C g^{-1} N	(p) C cost of N source 3
ϕ_4	9	g C g^{-1} N	(p) C cost of N source 4
Ψ_C	Variable	g C m^{-2} day^{-1}	(P) requirement for C
$\bar{\Psi}_C$	Variable	g C m^{-2} day^{-1}	(S) integrated requirement for C
Ψ_N	Variable	g N m^{-2} day^{-1}	(P) requirement for N
$\bar{\Psi}_N$	Variable	g N m^{-2} day^{-1}	(S) integrated requirement for N
ω	0.002	day^{-1}	(p) sub-effort allocation rate

N is subdivided among sub-efforts targeted at the resources that are potential sources of N (v_{Nk}; Eq. 1.5). The strategy to simulating the distribution of uptake effort is the heart of the modeling approach and is discussed in detail below (section titled "Allocation of uptake effort").

Allometry and stoichiometry: We use simple representation of allometric and stochiometric constraints on resource acquisition. Our allometric equation calculates the amount of plant biomass that is active in resource acquisition (S Eq. 1.17). We assume that the fraction of biomass active in resource acquisition declines as biomass increases and more structural tissues are added ($\alpha < \gamma$; Rastetter and Ågren 2002). This active biomass is used to calculate uptake of both C (Eq. 1.8) and the various sources of N (Eq. 1.10). We use a stoichiometric constraint (Θ) to help maintain a near optimum C:N ratio in the vegetation (Eq. 1.18) by adjusting respiration (Eq. 1.11) and N turnover (Eq. 1.13). In addition, the stoichiometric constraint is used to adjust the requirements for C and N so that uptake effort can be reallocated to help maintain the C:N ratio (Eqs. 1.15 & 1.16). To simplify interpretation of the simulations, we use a constant target C:N ratio (q_B), but a more complex representation can be substituted (e.g., one that changes the target C:N ratio with allometry).

Photosynthesis and N uptake: Both C and N acquisition are monotonically increasing functions of the biomass active in resource acquisition and of the effort allocated toward acquiring the resource. For photosynthesis we assume that, at the leaf level, photosynthesis increases as a rectangular hyperbola of irradiance (I) and integrate down through the canopy using a Beer's light extinction to calculate total-canopy photosynthesis (Eq. 1.8; Rastetter et al. 1992). The canopy leaf-area index (L_{AI}) increases with both the biomass active in resource acquisition (S) and with the effort expended toward C acquisition (V_C; Eq. 1.19). Uptake for each of the N sources (Eq. 1.10) is assumed to be a Michaelis-Menten function (Giese 1973) of the concentration of the N source in the environment (N_k) and proportional to the biomass active in resource acquisition (S), to the effort allocated toward N acquisition (V_N), and to the fraction of that effort allocated to that specific source of N (v_{Nk}).

Respiration and element turnover in biomass: We use a respiration equation with several terms (Eq. 1.11). The first term represents a baseline respiration that increases with both the biomass C (B_C) and the stoichiometric constraint (Θ). The remaining terms account for the cost of taking up and assimilating the various forms of N, calculated as the C cost per unit N uptake (ϕ_k) times the uptake of each N source (U_k).

Turnover of C and N represents the loss of plant tissues in litter. For C, we assume that the litter losses are simply proportional to the plant biomass C (Eq. 1.12; more complex equations accounting e.g., for allometry can be substituted). For N, litter losses are adjusted to decrease N loss if the biomass C:N is too high and increase N loss if the C:N is too low (Eq. 1.13).

Supply and loss of resources: As with the original MEL model (Rastetter and Shaver 1992), we are interested in the interaction between the idealized vegetation and the abundance and supply of resources, not in broader-scale controls on resources associated, for example, with ecosystem cycling. We therefore specify N supply rates (I_k) to drive the model (Eq. 1.3) regardless of whether the source is from outside the ecosystem or internally recycled within the ecosystem. We assume N losses from the environment are proportional to their concentration (Eq. 1.23). In one simulation, we assume one of the N sources is "non-depletable" (*sensu* Rastetter and Shaver 1992) and therefore control the concentration of the resource directly (specify N_k and Eq. 1.3 is ignored for that N source). We also assume the CO_2 taken up in photosynthesis is non-depletable.

Allocation of uptake effort: We calculate allocation of uptake effort hierarchically by first assessing primary uptake effort allocated toward C versus N (V_i; Eq. 1.4) and then partitioning the primary effort allocated to N among sub-efforts targeted toward the uptake of various substitutable sources of N (v_{ik}; Eq. 1.5). The primary effort represents the fraction of all uptake assets allocated to an element, thus, the V_i sum to one. Similarly, the sub-efforts represent fractions of these primary efforts allocated to various sources of a specific element and the sum of the v_{ik} over k is one.

We allocate effort between C and N based on the requirement relative to the uptake of each element (Eq. 1.4). The requirement is the rate of assimilation needed to replace elements lost in respiration and turnover but adjusted using the stoichiometric constraint (Θ) to compensate for past surpluses or deficiencies (Eqs. 1.15 & 1.16). Thus, we calculate the requirement for C like the calculation of respiration plus C turnover except that the stoichiometric constraint is in the numerator for respiration and in the denominator for the C requirement (Eq. 1.15). Similarly, the stoichiometric constraint is in the denominator for N turnover but in the numerator for the N requirement (Eq. 1.16). To avoid reallocation in response to high-frequency changes in the environment, we base reallocation (Eq. 1.4) on the time-integrated values of both requirement and uptake (Eqs. 1.6 & 1.7). This integration filters out high frequency changes in resource turnover and availability.

To assure that the primary efforts always sum to one, we multiply the requirement-to-uptake ratio in the allocation equation (Eq. 1.4) by a factor (Φ) equal to an effort-weighted geometric mean of the assimilation-to-requirement ratios (Eq. 1.14). Because of this factor, the redistribution of effort ceases when assimilation meets the same fraction of requirement for all elements (at steady state, $\bar{U}_i/\bar{\psi}_i = \Phi$·for all i). In this sense, allocation of effort drives the system toward a condition where all element resources are equally limiting (Chapin et al. 1987).

We partition the primary efforts among sub-efforts for substitutable N sources based on the relative values of their marginal yields of N per unit effort (y_{ik}; Eq. 1.5). The marginal yield is the incremental increase in N uptake per incremental increase in the total effort allocated toward that source of N. This total effort includes both the effort allocated directly toward the uptake of the resource plus any effort needed to acquire C (energy) consumed during the acquisition and assimilation of the N source. Thus, we calculate marginal yield (Eq. 1.24) as the incremental increase in the assimilation of N (ΔU_N) divided by the sum of the incremental increase in sub-effort needed to realize the increase in N acquisition ($V_N \Delta v_{Nk}$) and the effort needed to replace the C (energy) consumed because of the increase in resource uptake ($\Delta U_N \phi_k (dU_C/dV_C)^{-1}$).

To assure that the sub-efforts always sum to one, we calculate a term β (Eq. 1.21) that is used in the allocation equation (Eq. 1.5). This use of β in the allocation of sub-efforts (Eq. 1.5) is analogous to the use of Φ in the allocation of the primary efforts (Eq. 1.4).

Among the sources contributing toward the assimilation of N, allocation of sub-efforts is toward the source with the highest marginal yield of N (Eq. 1.5) and away from all other sources; only if the marginal yields are equal can the sub-efforts be sustained for more than one N source. The sub-efforts allocated to N sources with low marginal yield will asymptotically approach zero. If environmental conditions change, it is possible for the current allocation of sub-effort to an N source to be zero even if that source has the highest marginal yield ($v_{Nk} = 0$ and $y_{Nk} = y_{max}$). To start reallocation of sub-effort in such a case, we set the allocation equation proportional to a small initiation factor, ε_k, rather than to v_{Nk} (Eqs. 1.5, 1.21, & 1.22).

2.2. Model II: interdependent resources

Our model for illustrating interdependent resources is very similar to the model above and uses many of the same equations. The main differences are that Model II has only one source of N (Table 2, Eqs. 2.4, 2.15, & 2.21) and photosynthesis is calculated based on the interdependence of irradiance (I), atmospheric CO_2 (C_a), and soil water (W_s; Eqs. 2.10 - 2.13). The model runs on a 0.1-hour time step. Here we only describe equations that differ from those in Model I.

Water budget: To simulate the water budget we include mass balance equations for both canopy (W_c) and soil water (W_s) storage (Eqs. 2.3 & 2.5). The canopy budget is based on water uptake (U_W) and

Table 2
Model II equations for interdependent resources. Variable and parameter values and definitions below equations.

2.1	$\frac{dB_C}{dt} = U_C - T_C - R_C$	2.2	$\frac{dB_N}{dt} = U_N - T_N$
2.3	$\frac{dW_c}{dt} = U_W - T_R$	2.4	$\frac{dN}{dt} = I_N - U_N - L_N$
2.5	$\frac{dW_s}{dt} = P_{pt} - U_W - R_O$	2.6	$\frac{dV_i}{dt} = a\ \ln(\Phi\ \frac{\Psi_i}{\bar{U}_i})\ V_i$
2.7	$\frac{dv_{Ck}}{dt} = \omega g(\frac{y_{Ck}}{y_{max}} - \beta) v_{Ck}$	2.8	$\frac{d\Psi_i}{dt} = \rho(\Psi_i - \bar{\Psi}_i)$
2.9	$\frac{d\bar{U}_i}{dt} = \rho(U_i - \bar{U}_i)$	2.10	$U_C = \min(U_{CI},\ U_{CCa},\ U_{CW})$
2.11	$U_{CI} = \frac{P_{Imax}}{k_I} \ln\{\frac{\eta + I}{\eta + Ie^{-k_I L_{AI}}}\}$	2.12	$U_{CCa} = \frac{P_{Cmax} C_a}{k_C + C_a}\ L_{AI}$
2.13	$U_{CW} = L_{AI}\ P_W\ (\psi_c - \psi_w)\ C_a$	2.14	$U_W = S\ g_W(\psi_s - \psi_c) V_C v_{CW}$
2.15	$U_N = S\ \frac{g_N\ N}{k_N + N}\ V_N$	2.16	$T_N = \frac{m_N\ B_N}{\Theta}$
2.17	$T_C = m_C\ \ B_C$	2.18	$R_C = r_C\ \Theta\ B_C$
2.19	$T_R = \frac{\sigma\ U_C\ V_{PD}}{C_a(1 + V_{PD}\ /\ V_0)}$	2.20	$R_O = \tau_W(W_s - W_f)$ if $W_s > W_f = 0$ otherwise
2.21	$L_N = \tau_N N$	2.22	$L_{AI} = \lambda\ S\ V_C(v_{CCa} + v_{CI})$
2.23	$P_{Imax} = \frac{\rho_I\ v_{CI}}{v_{CCa} + v_{CI}}$	2.24	$P_{Cmax} = \frac{\rho_C\ v_{CCa}}{v_{CCa} + v_{CI}}$
2.25	$\Psi_C = \frac{(r_C + m_C)\ B_C}{\Theta}$	2.26	$\Psi_N = m_N\ \Theta\ B_N$
2.27	$\psi_s = -0.01(\frac{W_s}{W_f})^{-b}$	2.28	$\psi_c = \psi_w + \frac{W_c}{c\ L_{AI}}$
2.29	$S = B_C(\frac{\alpha B_C + 1}{\gamma B_C + 1})$	2.30	$\Theta = \frac{B_C}{B_N q_B}$
2.31	$\beta = \frac{\sum_k(y_{Ck}\ v_{Ck})}{y_{max}\ \sum_k(v_{Ck})}$	2.32	$y_{max} = max(y_{Ck})$
2.33	$y_{Ck} = \frac{1}{V_C}\ \frac{dU_C}{dv_{Ck}}$	2.34	$\Phi = \prod_i (\frac{\bar{U}_i}{\bar{\Psi}_i})^{V_i}$
2.35	$\frac{dU_C}{dv_{CW}} = \frac{U_C}{T_R}\ \frac{dU_W}{dv_{CW}}$		

Variables and Parameters (for i = C or N; k = I, Ca, or W) . In description, (p) – parameter, (S) – state variable, (P) – process variable, (D) – driver variable.

Symbol	value	units	description
a	0.00008	hr^{-1}	(p) effort allocation rate
b	5	none	(p) water potential exponent
B_C	Variable	g C m^{-2}	(S) vegetation C
B_N	Variable	g N m^{-2}	(S) vegetation N
c	0.144	MPa mm^{-1}	(p) canopy water capacitance
C_a	Variable	µmol CO_2 mol^{-1}	(D) atmospheric CO_2
g_N	0.0000539	g N g^{-1}C hr^{-1}	(p) N uptake rate constant
g_W	0.0516	mm g^{-1}C MPa^{-1} hr^{-1}	(p) water uptake constant
I		Variable µmol m^{-2} sec^{-1}	(D) irradiance
I_N	Variable	g N m^{-2} hr^{-1}	(D) N inputs
k_C	400	µmol CO_2 mol^{-1}	(p) CO_2 half-saturation constant
k_I	0.5	m^2 m^{-2}	(p) Beer's coefficient
k_N	1	g N m^{-2}	(p) N half saturation
L_{AI}	Variable	m^2 m^{-2}	(P) leaf area index
L_N	Variable	g N m^{-2} hr^{-1}	(P) N loss
m_C	0.0000167	hr^{-1}	(p) C turnover coefficient
m_N	0.0000505	hr^{-1}	(p) N turnover coefficient
N	Variable	g N m^{-2}	(S) available N
P_{Cmax}	Variable	g C m^{-2} hr^{-1}	(P) maximum CO_2-limited photosynthesis
P_{Imax}	Variable	g C m^{-2} hr^{-1}	(P) maximum light-limited photosynthesis
P_{pt}	Variable	mm hr^{-1}	(D) rainfall
P_W	0.000381	g C mol µmol^{-1} CO_2 m^{-2} leaf hr^{-1} MPa^{-1}	(p) Water-limited photosynthesis rate constant
q_B	152	g C g^{-1} N	(p) biomass optimum C:N ratio
r_C	0.0000167	hr^{-1}	(p) respiration coefficient
R_C	Variable	g C m^{-2} hr^{-1}	(P) respiration
R_o	Variable	mm hr^{-1}	(P) runoff
S	Variable	g C m^{-2}	(P) biomass active in uptake
T_C	Variable	g C m^{-2} hr^{-1}	(P) C turnover in litter
T_N	Variable	g N m^{-2} hr^{-1}	(P) N turnover in litter
T_R	Variable	mm hr^{-1}	(P) transpiration
U_C	Variable	g C m^{-2} hr^{-1}	(P) uptake of C
$\bar{U}_C$	Variable	g C m^{-2} hr^{-1}	(S) integrated uptake of C
U_{CCa}	Variable	g C m^{-2} hr^{-1}	(P) CO_2-limited photosynthesis
U_{CI}	Variable	g C m^{-2} hr^{-1}	(P) light-limited photosynthesis
U_{CW}	Variable	g C m^{-2} hr^{-1}	(P) Water-limited photosynthesis
U_N	Variable	g N m^{-2} hr^{-1}	(P) uptake of N
$\bar{U}_N$	Variable	g N m^{-2} hr^{-1}	(S) integrated uptake of N
U_W	Variable	mm hr^{-1}	(P) Water uptake
V_C	Variable	none	(S) effort toward C
V_N	Variable	none	(S) effort toward N
V_0	0.00167	MPa	(p) VPD constant
v_{Ck}	Variable	none	(S) sub-effort toward C interdependent resource k
V_{PD}	Variable	MPa	(D) vapor pressure deficit

(*continued on next page*)

Table 2 (*continued*)

2.1	$\frac{dB_C}{dt} = U_C - T_C - R_C$			2.2	$\frac{dB_N}{dt} = U_N - T_N$
W_c	Variable	mm			(S) canopy water
W_f	100	mm			(p) field capacity
W_s	Variable	mm			(S) soil water
y_{Ck}	Variable	g N m^{-2} hr^{-1}			(P) marginal yield from interdependent resource k
y_{max}	Variable	g N m^{-2} hr^{-1}			(P) maximum marginal yield of C
α	0.000006	m^2 g^{-1}C			(p) allometric constant
β	Variable	none			(P) sub-effort balance correction
γ	0.0045	m^2 g^{-1}C			(p) allometric constant
η		600	μmol m^{-2} sec^{-1}		(p) irradiance half saturation constant
Θ	Variable	none			(P) stoichiometric constraint
λ	0.0282	m^2 g^{-1}C			(p) specific leaf area
ρ	0.00008	hr^{-1}			(p) uptake & requirement integration constant
ρ_C	0.882	g C m^{-2} leaf hr^{-1}			(p) maximum CO_2-limited leaf photosynthesis
ρ_I	0.99	g C m^{-2} leaf hr^{-1}			(p) maximum light-limited leaf photosynthesis
σ	969,000	L mmol CO_2 MPa g^{-1}C mol^{-1}			(p) transpiration constant
τ_N	0.015	hr^{-1}			(p) n loss parameter
τ_W	0.02	hr^{-1}			(p) water loss parameter
Φ	Variable	none			(P) weighted geometric mean uptake:requirement
ψ_c	Variable	MPa			(P) canopy water potential
Ψ_C	Variable	g C m^{-2} hr^{-1}			(P) requirement for C
$\bar{\Psi}_C$	Variable	g C m^{-2} hr^{-1}			(S) integrated requirement for C
Ψ_N	Variable	g N m^{-2} hr^{-1}			(P) requirement for N
$\bar{\Psi}_N$	Variable	g N m^{-2} hr^{-1}			(S) integrated requirement for N
ψ_s	Variable	MPa			(P) soil water potential
ψ_w	-2.50	MPa			(p) wilting potential
ω	0.00210	hr^{-1}			(p) sub-effort allocation rate

transpiration (T_R) and the soil water budget is based on precipitation (P_{pt}), uptake (U_W), and runoff plus deep percolation (R_O). Water uptake is proportional to the biomass active in resource acquisition (S), the water potential difference between soil and canopy ($\psi_s - \psi_c$), and the effort allocated toward water acquisition (V_C v_{CW}; Eq. 2.14). Soil water potential is calculated as a power function of the ratio of soil water to field capacity (Eq. 2.27; Clapp and Hornberger 1978). We assume canopy potential above wilting (ψ_c - ψ_w) is proportional to canopy water (W_c) and inversely proportional to leaf area times a canopy capacitance (c L_{AI}; Eq. 2.28, Williams et al. 1996). Transpiration is simulated using a modified Ball-Berry-Leuning model (Leuning 1995; Eq. 2.19). Transpiration is proportional to C assimilation (U_C), inversely proportional to CO_2 concentration (C_a), and increases asymptotically with vapor pressure deficit (V_{PD}). Runoff and deep percolation is proportional to the soil water content above the field capacity ($W_s - W_f$; Eq. 2.20).

Photosynthesis: Photosynthesis (U_C) is calculated as the minimum of a light-limited rate (U_{CI}), a CO_2-limited rate (U_{CCa}), and a water-limited rate (U_{CW}; Eq. 2.10). The light-limited rate of photosynthesis is calculated in the same way as in Model I (Eq. 2.11) except the maximum leaf-level rate (P_{Imax}) is based on the sub-effort distribution between light capture and carboxylation (Eq. 2.23). The CO_2-limited rate (Eq. 2.12) is proportional to leaf area (L_{AI}), to a Michaelis-Menten function of CO_2 (C_a), and to a maximum leaf-level rate (P_{Cmax}) adjusted based on sub-effort allocation between light capture and carboxylation (Eq. 2.24). The leaf-area index is calculated based only on the fraction of C effort allocated to light and CO_2 (i.e., allocation of water is not included; Eq. 2.22). The water-limited rate of photosynthesis is proportional to L_{AI}, to CO_2 (C_a), and to the canopy water potential above wilting ($\psi_c - \psi_w$; Eq. 2.13).

Other changes: Because light, CO_2, and water are treated as interdependent resources in the production of a single product, carbohydrate, no relative differences in cost can be assessed and we set the assimilation costs to zero ($\phi_i = 0$). This common cost among interdependent resources simplifies several equations; the marginal yield equation is simply the change in C uptake per change in effort (Eq. 2.33) and the acquisition costs are removed from the calculation of respiration (Eq. 2.18) and C requirement (Eq. 2.25).

Because the resources are interdependent, at least some effort must always be allocated to all three resources. The v_{Ci} therefore never decay to zero, alleviating the need for ε_i in the allocation equation for sub-efforts (Eq. 2.7) and in the correction term used to maintain the sum of sub-efforts at one (Eq. 2.31).

Finally, the effort allocated toward water does not have a direct effect on photosynthesis, but rather affects photosynthesis indirectly through the supply of water to the canopy. It is therefore difficult to assess the marginal yield of carbohydrate from effort allocated to water. We solve this issue by calculating marginal yield as the water-use efficiency for photosynthesis (U_C / T_R) times the marginal yield of water uptake from effort allocated toward water (dU_W / dv_{CW}; Eq. 2.35).

3. Analyses

3.1. Substitutable resources

Substitutability of two resources: We run several simulations with the substitutable resource model using daily drivers (Model I; Table 1). In the first, we analyze substitutability between two N sources in the context of Tilman's (1982) graphic analysis. We use the model to find the supply rate of the more expensive N source that is needed to maintain specified rates of net primary production (NPP = $U_C - R_C$) or gross primary production (GPP = U_C) to determine if two N sources in our model are "perfectly substitutable" (*sensu* Tilman 1982).

Tilman (1982) illustrates substitutability between two resources using production isoclines on a graph where the two axes are the supply rates of the two resources. If resources are perfectly substitutable then the isoclines are straight lines running from upper left to lower right on the graph. For our model, N resources are perfectly substitutable for NPP isoclines (Fig. 1 upper panel). The slope of these isoclines increases with the cost of the resource plotted on the vertical axis. This increased slope results from the need to allocate more effort to acquire C to cover the increased cost of N acquisition. To increase the effort toward C, the effort toward N must decrease, which can only happen if the availability of the N resource increases so that it can be acquired with less effort. The increased availability can only be achieved with a higher N supply rate. Hence the steeper slope of the NPP isocline.

For GPP isoclines, N resources in our model are not perfectly

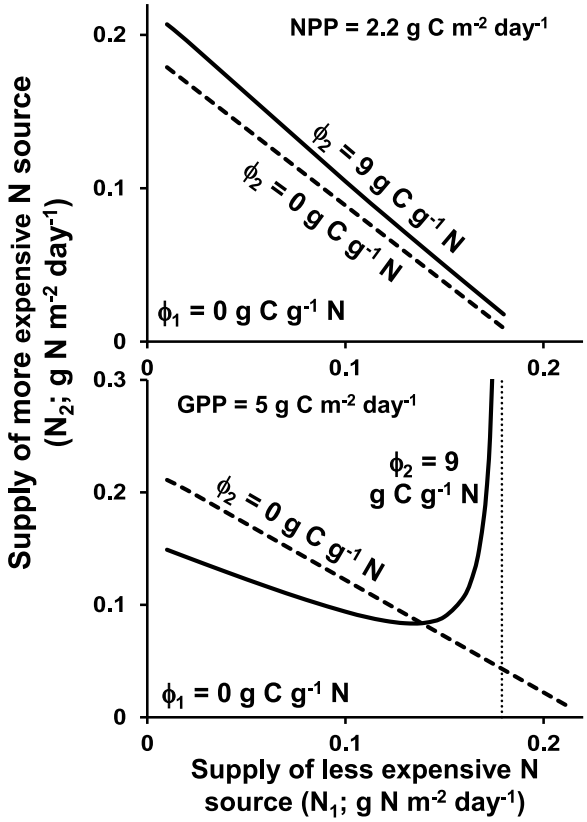

Fig. 1. Assessment of substitutability. When assessed for net primary production (NPP), N resources in our model are perfectly substitutable regardless of relative cost (strait diagonal NPP isoclines in upper panel). The slope of the NPP isoclines steepens as the difference in relative cost of the two substitutable resources increases. When assessed for gross primary production (GPP), N resources in our model are perfectly substitutable only under specific conditions like when their cost (ϕ_k) and uptake rate constant (g_k) are equal (dashed line in lower panel). If the cost of the more expensive N source is too high or its uptake potential per unit effort it too low (solid curve in lower panel), then there is a supply rate for the less expensive N source above which no supply rate of the more expensive resource can maintain GPP for the specified isocline (vertical dotted line in lower panel).

substitutable except under limited conditions (e.g., $\phi_1 = \phi_2$ and $g_1 = g_2$; Fig. 1 lower panel). Under most conditions the GPP isoclines diverge from those expected for perfectly substitutable resources at high supply rates of the less expensive of the resources (right side of graph). As the supply of the less expensive resource increases, the supply rate of the more expensive resource will first decrease, consistent with perfect substitution, but will then increase toward a vertical asymptote if the cost (ϕ_k) of the more expensive resource is high enough and its uptake rate constant (g_k) low enough. Because two N sources can be simultaneously exploited in our model only when their marginal yields (Eq. 1.24) are equal ($y_1 = y_2$), this asymptote means that there is a supply rate for the less expensive N source (N_1) above which the marginal yield for the more expensive N source (N_2) is less than that of N_1 even when the availability of N_2 is saturating ($y_2 < y_1$ even when $N_2/(k_2 + N_2) = 1$). The availability of the less expensive N source at this asymptote ($y_1 = y_2$ and $\lim\{N_2/(k_2 + N_2)\} \rightarrow 1$) is

$$N_{1A} = \frac{g_2 k_1}{g_1 - g_2 + g_1 g_2 S(\phi_2 - \phi_1)\left(\frac{dU_C}{dV_C}\right)^{-1}}$$

where the A in the subscript indicates the availability of N_1 at the asymptote. If N_{1A} is less than the availability of N_1 where its supply rate alone is enough to support production at the GPP isocline, then the asymptote will leave a gap at the right side of the graph where no rate of supply for N_2 will yield the GPP of the specified isocline (Fig. 1 lower panel).

To understand this dynamic, consider the case where the supply rate of the N_1 is exactly enough to support the GPP of the specified isocline. If the supply rate of N_1 is then decreased by a small amount, the GPP will decrease unless the N shortfall can be made up by increasing the uptake of N_2. The effort-allocation algorithm will only allow this reallocation toward the more expensive N source if the NPP increases. If the supply rate of N_2 is not high enough both (a) to compensate for the N shortfall left by decreasing the supply of N_1 and (b) to allow enough effort to be reallocated from N to C to cover the extra cost of using N_2, then the GPP cannot be maintained at the specified isocline. If the availability of N_2 cannot meet these two criteria even if the uptake mechanism is saturated ($N_2 >> k_2$), then there is no supply rate that is high enough to meet the two criteria.

This difference between substitutability from the perspectives of NPP and GPP are consistent with the resource optimization paradigm underlying our model (Chapin et al. 1987). The cost of N uptake is incorporated into the calculation of NPP, but not of GPP. Because this cost is intrinsic to the optimization of effort allocation, the two N sources appear perfectly substitutable from the perspective of NPP but not of GPP.

Use of substitutable N sources during vegetation development: In another analysis, we simulate the development of vegetation with four sources of N. The input rates (I_k) and values for all the parameters associated with these N sources are identical (g_k, k_k, & τ_k) except for the acquisition costs (ϕ_k), which are set so that cost increases from N source 1 to 4 ($\phi_1 < \phi_2 < \phi_3 < \phi_4$; Table 2). All four N sources are required to maintain the mature vegetation.

Initially the vegetation allocates all its N acquisition effort toward N source 1, the least expensive of the N sources (Fig. 2). However, the rate of uptake quickly exceeds the rate of supply, the amount of N source 1 declines (Fig. 2), and the marginal yield for source 1 drops below that of source 2 (Fig.3), the second least expensive N source. The vegetation therefore reallocates effort from N source 1 to N source 2, the abundance of N source 1 recovers slightly and the marginal yields for N sources 1 and 2 converge. As the vegetation uses N source 2, its abundance and marginal yield decline and the vegetation reallocates effort toward N source 3. This sequence continues until all four N sources are used and their marginal yields converge on the same value. Although the marginal yields converge, the abundances and sub-efforts do not converge on the same values. Eventually the system approaches a steady state where the abundances of less expensive N sources are lower than the abundances of more expensive N sources ($N_1 < N_2 < N_3 < N_4$; Fig. 2 center panel) and the sub-efforts allocated to less expensive N sources are higher than sub-efforts allocated to more expensive N sources ($v_{N1} > v_{N2} > v_{N3} > v_{N4}$; Fig. 2 bottom panel). The C:N ratio of the biomass is maintained within tight constraints in the simulation but deviates toward high N concentrations during the transitions among N sources as the vegetation adapts to ever increasing C costs of the N taken up.

The lags between the initiations of use for successive N sources is only partly caused by the increasing costs of acquisition among the N sources. As the abundance of an N source drops, its marginal yield also drops. Once that marginal yield drops below the marginal yield of the next N source in the sequence, it triggers the reallocation toward the next least expensive N source. However, most of the lag in the simulations results from the time it takes to reallocate effort from one source to the next. Such lags are expected of real biological systems and would not be captured using standard *optimized*, as opposed to our *optimizing*, approach. The rate of acclimation can be adjusted using the rate parameters a and ω (Eqs. 1.4 & 1.5).

The preferential use of less expensive N sources before more expensive sources are exploited is consistent with the resource optimization paradigm underlying our model. As expected, each N source is depleted until its marginal yield declines below that of the next N

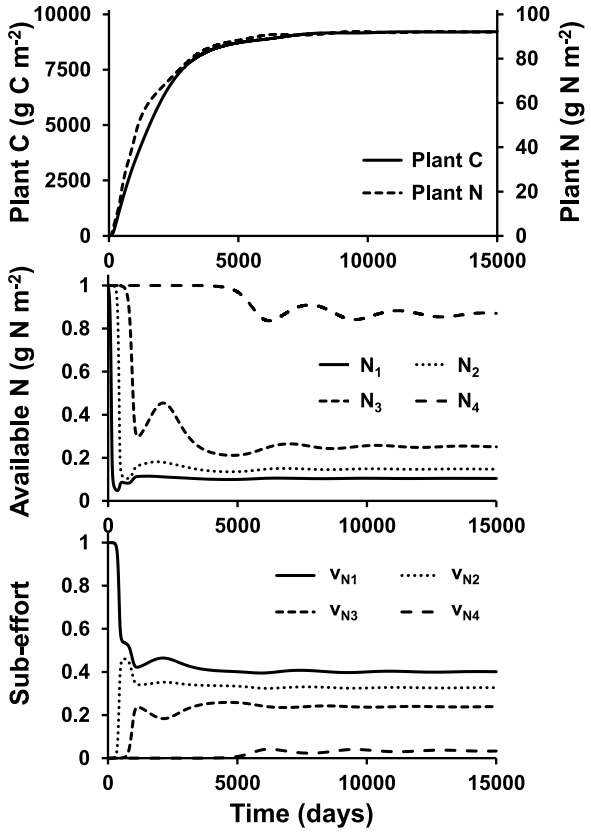

Fig. 2. Plant growth on four substitutable sources on N. As C and N accumulate in plant biomass (upper panel), the plant exploits the least expensive N source first (N_1), then used progressively more expensive N sources ($N_2 < N_3, < N_4$) as less expensive sources get depleted (center panel). Exploitation of successive N sources is accomplished by redistributing the sub-effort allocated to the uptake of each N source (bottom panel).

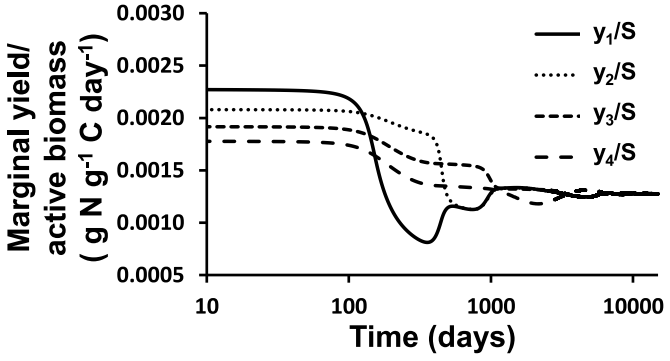

Fig. 3. Marginal yield of N uptake per unit active biomass for four substitutable N sources as plant biomass accumulates (shown in Fig. 2). Marginal yield is the incremental increase in N uptake per incremental increase in effort expended. The effort expended includes both the effort allocated directly to N uptake and the effort allocated to acquire C to support the energy costs of N uptake and assimilation. These energy costs increase from N source 1 (lowest cost) to N source 4 (highest cost).

source in the sequence. In the end, the concentrations of the four N sources are depleted to the level where their marginal yields converge on the same value.

To assess the degree of limitation by each of the N sources, we run four simulations in which we make each of the four N sources unavailable to the vegetation, one at a time. Relative to the previous simulation (control), making the least expensive N source unavailable results in over a 6% drop in the steady-state biomass and almost a 6%

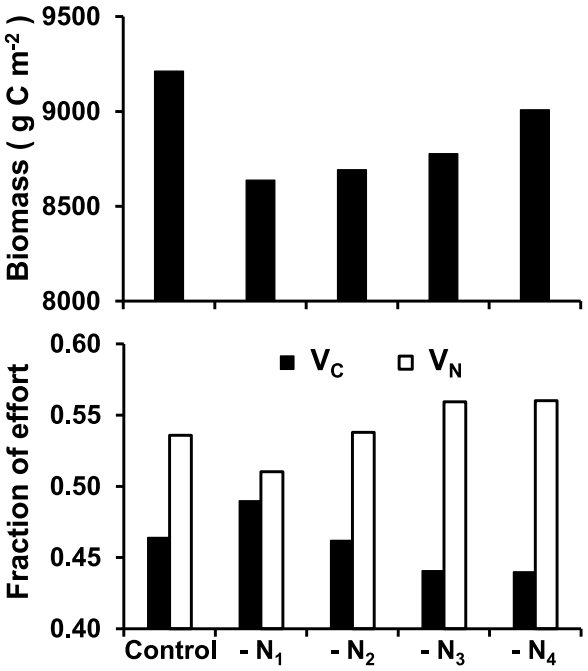

Fig. 4. Steady-state biomass and effort distribution between C and N uptake in simulations with all four N sources available (control) and with each of the four N sources made unavailable. Removing any of the N sources decreases biomass relative to the control but removing the least expensive N source ($-N_1$) results in the largest biomass loss and removal of the most expensive N source ($-N_4$) results in the smallest biomass loss. As progressively more expensive N sources are made unavailable, less effort is needed to cover the C cost of N uptake and the C effort (V_C) declines and is reallocated toward N uptake (V_N).

increase in effort allocated to C acquisition to compensate for the extra cost of assimilating the other, more expensive N sources ($-N_1$ in Fig. 4). Making each of the other N sources unavailable also results in a drop in steady-state biomass relative to the control, but that drop is progressively less for progressively more expensive N sources; making the most expensive N source unavailable resulted in just over a 2% decrease in biomass relative to the control. This pattern in the steady-state biomasses is of course related to the amount of each N source used in the control simulation, with the least expensive source contributing the highest fraction of the total N uptake and the most expensive contributing the least. However, the pattern is also related to the redistribution of uptake effort between C and N. Consistent with the resource optimization paradigm, as progressively more expensive N sources are made unavailable, progressively less effort needs to be allocated to C to compensate for the acquisition cost. This decrease in C effort results in a commensurate increase in N effort, which in turn partly compensates for the loss of the N source. The control distribution of effort is intermediate among the distributions where a N source was made unavailable; the control C effort is higher than when the least expensive source is unavailable but lower than when the two most expensive N sources are unavailable.

Use of substitutable N sources during vegetation development when one source is not depletable: Conditions for the next simulation are identical to those in the 4-N source simulation above except that the abundance of N source 3 is held constant at 1 g N m^{-2} (N_3 is non-depletable *sensu* Rastetter and Shaver 1992). Dynamics are identical to those in the 4-N source simulation until the marginal yield for N source 2 drops below that of N source 3 (Figs. 5 and 6). Because the abundance of N source 3 cannot decline as it is taken up by the vegetation, the decline in marginal yield for N source 3 is smaller than in the previous simulation (Fig. 6). The relative costs of the various N sources, the non-depletability of N source 3, and the high marginal yield for N source 3 result in the effort allocated to N source 3 being higher than N source 2, but

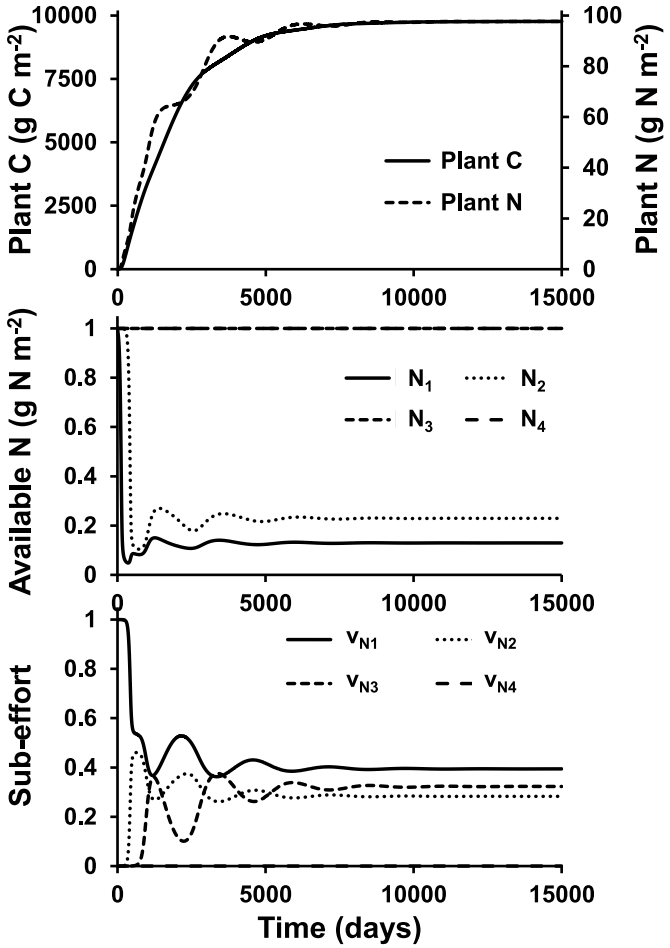

Fig. 5. Plant growth when the third N source (N_3) is held constant at 1 g N m^{-2} (non-depletable). Conditions are otherwise identical to those in Fig. 2. The plant can fill its N requirement from sources N_1, N_2, and the effectively infinite source, N_3 and therefore does not use the most expensive N source, N_4. The non-depletability of N source 3 partly compensates for its high cost so that more effort is allocated toward it than to N source 2.

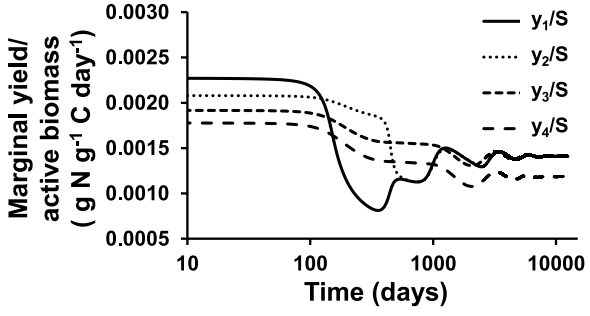

Fig. 6. Marginal yield of N uptake per unit active biomass when N source 3 is not depletable. Conditions are otherwise identical to those in Fig. 3.

not as high as N source 1 (Fig. 5). The vegetation never uses N source 4. The non-depletability of N source 3, the high yield for N source 3, and the consequent lack of need for the expensive N source 4 results in a steady-state biomass that is 6% higher than in the 4-N source simulation. Again, the lags in the dynamics are mostly the result of the time it takes to reallocate effort.

These results are again consistent with the resource optimization theory underlying the model. With a non-depletable N source, the marginal yield cannot drop as a result of decreases substrate concentration. Nevertheless, the marginal yield for all the N sources that are exploited converge on the same value. The marginal yield for the N source that is not used remains below that of the other N sources.

N fixation as a substitutable source of N: In the final simulation with this model, we model vegetation development with symbiotic N fixation. In an earlier version of the MEL model (Rastetter et al. 2001), N fixation was assumed to have a fixed C cost and that cost was compared to the cost of N uptake assessed as the loss in photosynthesis per unit gain in N uptake as a result of reallocation of effort from canopy to roots: cost of N uptake = $(dU_C/dV_C)/(dU_N/dV_N)$ (both N-fixation and N-uptake costs in units of g C g^{-1} N). Symbiotic N fixation increased in proportion to the N-uptake cost minus the N-fixation cost. This earlier approach does not incorporate N fixation into the allocation algorithm directly; N fixation is therefore an add-on to the C-N optimization approach. With substitutable resources, N fixation can be incorporated directly into the allocation algorithm.

We assume N fixation is proportional to the biomass active in uptake and to allocated effort:

$$U_{Nfix} = g_{fix}\ S\ V_N v_{fix}$$

where g_{fix} = 0.00064 g N g^{-1}C day^{-1} and the N-fixation cost ϕ_{fix} = 9 g C g^{-1} N. Instead of four sources of available N in the soil, we assume only a single source of N, which is taken up using the same uptake equation used in the previous simulations (Eq. 1.10) but we set the rate constant for N uptake and the N-loss parameter to four times their values in the previous simulations (g_{Nup} = 0.01, t_N = 0.28) and set the acquisition cost to zero (ϕ_N = 0 g C g^{-1} N); to compensate for the lower cost we lower P_{max} from 4 to 3. We initialize the simulation with all the N sub-effort allocated toward N fixation (v_{fix} = 1) and the abundance of available N in the soil set to zero. To mimic the increase in N mineralization as soil stocks accumulate, we increase the supply rate of available N (I_N) linearly from 0 to 0.28 g N m^{-2} day^{-1} over 15,000 days; this final supply rate is equal to the sum of the supply rates for all four N sources in the previous simulations.

Initially the vegetation relies exclusively on N fixation and the rate of fixation increases as the biomass increases (Fig. 7). However, with the increasing rate of N supply we impose on the simulation, the marginal yield for N uptake exceeds that of N fixation within about 100 days (Fig. 8). Because of the time required to reallocate effort, effort allocated to N fixation continues to exceed that allocated to N uptake for about the first 2500 days and the N fixation rate exceeds the N uptake rate (Fig. 7). Available N in the soil increases for about 260 days then declines as biomass and N demand increase (not shown). The marginal yield for N uptake declines as N availability drops but levels off at a slightly higher value than that for N fixation (Fig. 8). By about day 6000, N supply exceeds N demand and available N again begins to accumulate, the marginal yield for N uptake increases while that of N fixation declines, and N fixation effectively stops. Relieved of the high cost of N fixation and because of the increasing rate of N supply, the vegetation can accumulate C faster (Fig. 7). At steady state with a N supply rate of 0.28 g N m^{-2} day^{-1}, the N sub-effort is allocated almost exclusively to N uptake and, with a zero C cost of N acquisition, the vegetation levels off at a biomass about 8% higher than in the previous simulations.

Symbiotic N fixation in most temperate and boreal forests is restricted to early phases of succession (Cleveland et al. 1999, Crews 1999). As with our earlier work (Rastetter et al. 2001), our results here indicate that this temporal pattern of symbiotic N fixation is consistent with the resource optimization paradigm. Once the canopy closes and the supply of internally cycled N increases sufficiently, it is just too expensive to continue symbiotic N fixation.

3.2. Interdependent resources

Acclimation of photosynthesis to interdependent light, CO_2, and water resources: We use one calibration of the interdependent model with sub-

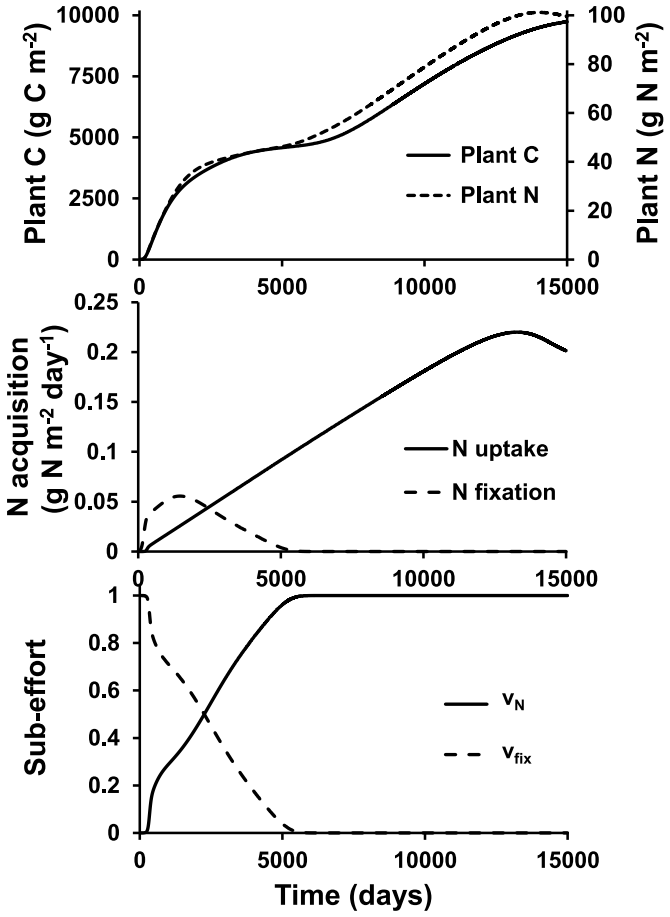

Fig. 7. Plant growth on soil N and symbiotic N fixation. Soil N is initially zero but the supply of N to the soil increases linearly over time. Because there is no soil N initially, the plant relies entirely on N fixation despite its high expense. As N builds up in the soil, the plant relies more and more on soil N (center panel) and reallocates effort from N fixation to the less expensive uptake of soil N (lower panel). Relieved of the high cost of N fixation (~ 6000 days), the plant can grow faster (upper panel).

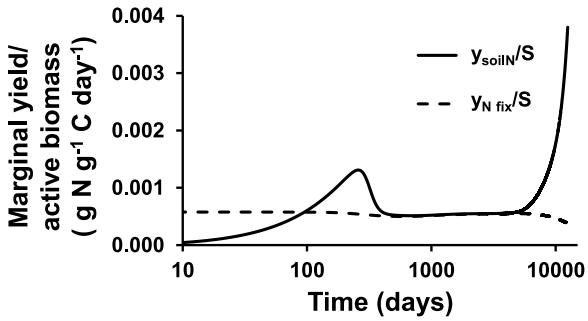

Fig. 8. Marginal yield of N uptake per unit active biomass with a soil N source and symbiotic N fixation.

hourly drivers (model II; Table 2) but allow the modeled vegetation to acclimate under five environmental conditions. In all simulations, the N input is held constant at 0.015 g N m^{-2} hr^{-1}. Under our control conditions, we simulate irradiance using the positive half of a sine wave with zero irradiance before 6 am and after 6 pm and peak irradiance of 1500 μmol m^{-2} sec^{-1} at noon, we hold CO_2 constant at 400 μmol mol^{-1}, we hold soil water constant at -0.01 MPa water potential (field capacity), and we vary vapor pressure deficit as a full sine wave with a minimum of zero (dew point) at 3 am and a maximum of 3.56×10^{-4} MPa (~90% humidity at 25 °C) at 3 pm. For dry-soil conditions, we use the same conditions as in the control except we hold soil water at -1 MPa water potential. For dry-air conditions, we again use the same conditions as in the control but increase the amplitude of the vapor pressure deficit sine wave so that the maximum is 0.0017 MPa (~ 50% humidity at 25 °C) at 3 pm. For high CO_2 conditions, we hold CO_2 at 600 μmol mol^{-1}. Finally, for low light conditions, we decrease the amplitude of the truncated sine wave for irradiance so that the peak irradiance at noon is only 900 μmol m^{-2} sec^{-1}.

At steady state, vegetation biomass under the five environmental conditions range from 5000 g C m^{-2} to 8385 g C m^{-2} (Table 3). Dry soil is the least favorable condition and has the lowest biomass followed by low light, dry air, control, and high CO_2. Daily photosynthesis and net primary production follow the same ranking. At steady state, under all five environmental conditions, the vegetation C:N ratio was 151.5 g C g^{-1} N, indicating that the model can allocate effort among resources to maintain the same stoichiometric balance under all five environmental conditions.

Under the control conditions, effort is allocated almost evenly between C and N (Fig. 9). The C effort is then partitioned among the three interdependent resources, light, CO_2, and water. Because the water supply is high (moist soil) and the water demand low (moist air), very little of the C effort is allocated toward water (< 3% of the total effort; Fig. 9). Slightly more of the remaining C effort is allocated to light than to CO_2. For the twelve hours of daylight, the allocation of C effort results in photosynthesis being limited for about 4 h each by light, CO_2, and water (Fig. 10, Table 3).

Relative to the control conditions, each of the other conditions to which the model acclimates results in a reallocation of effort among the four resources. The dry soil imposes a severe water limitation and effort is reallocated away from N, light, and CO_2 until over 40% of the total effort is allocated to water (Fig. 9). A dry atmosphere also imposes a water limitation, but because of the moist soil the limitation is far less severe and the reallocation of effort away from N, light, and CO_2 is much smaller with only 8% of the steady-state effort allocated to water. Elevated CO_2 both alleviates CO_2 limitation and increases water-use efficiency (Table 2 Eq. 2.19); reallocation is therefore away from CO_2 and water, very slightly toward light, but mostly toward N. Low light results in a reallocation of effort away from N, CO_2, and water and toward light. As with the control conditions, acclimation to the other simulated conditions results in the reallocation of C effort among the three interdependent resources such that photosynthesis is limited for about 4 h each by light, CO_2, and water over the 12 h of daylight (Fig. 10, Table 3). These distributions of effort under the five conditions are consistent with the resource optimization paradigm.

Surprisingly, the afternoon decline in photosynthesis associated with canopy water limitation (stomatal closure; Table 2 Eq. 2.13) is smallest in the acclimation to dry soil and dry air (Fig. 10). This decline in afternoon water limitation is partly the result of lower allocation to light and CO_2 acquisition so over all photosynthesis is lower and partly the result of the high allocation to water acquisition, which increases the rate of water transfer from the soil to the canopy. This connectivity between soil and canopy is particularly strong in the acclimation to dry soil, which results in a very high allocation of effort toward water acquisition, a low leaf area (Table 2 Eq. 2.22), and therefore a low canopy water-holding capacity (Table 2 Eq. 2.28). Because water flows rapidly through the vegetation and the canopy water storage capacity is small, there is a much smaller cycle of canopy recharge and discharge.

Initial responses to changes in interdependent light, CO_2, and water resources: We run the model acclimated to each of the five environmental conditions for one 24-h period under all five of the environmental conditions (Table 3). In all simulations where the model is run under the same condition to which it was acclimated, the daily nitrogen-use efficiency of photosynthesis (NUE_{GPP} = photosynthesis/N uptake) is 100 ± 0.2 g C g^{-1} N, the daily nitrogen-use efficiency of net primary production (NUE_{NPP} = [photosynthesis – respiration]/ N uptake) is 50 ± 0.2 g C g^{-1} N, and the photosynthesis is limited for four hours

Table 3
Modeled biomass after acclimation to control, dry soil, dry air, high CO_2, and low light conditions and metabolism over 24 h under the same five conditions. Biomass C and N in g m^{-2}, GPP – gross primary production (g C m^{-2} day^{-1}); NPP – net primary production (g C m^{-2} day^{-1}); ET – transpiration (mm day^{-1}); U_N – N uptake (g N m^{-2} day^{-1}); WUE – water-use efficiency (= GPP/ET); NUE_{GPP} – N-use efficiency for GPP (= GPP/U_N); NUE_{NPP} – N-use efficiency for NPP (= NPP/U_N); L/C/W – hours of GPP limitation by light, CO_2, and water.

			24-hour simulation condition				
Acclimation condition	Biomass	Metabolism	Control	Dry soil	Dry air	High CO_2	Low light
Control	C = 7991	GPP	6.39	4.55	3.91	7.47	5.67
	N = 52.74	NPP	3.19	1.35	0.71	4.27	2.47
	C:N = 151.5	ET	3.47	2.36	6.40	2.77	3.18
		U_N	0.06	0.06	0.06	0.06	0.06
		WUE	1.84	1.93	0.61	2.70	1.78
		NUE_{GPP}	**99.84**	71.09	61.09	116.72	88.59
		NUE_{NPP}	**49.84**	21.09	11.09	66.72	38.59
		L/C/W	**4/4/4**	3/0/9	3/0/9	7/5/0	8/2/2
Dry soil	C = 5000	GPP	4.02	4.00	4.01	4.56	3.58
	N = 33.00	NPP	2.02	2.00	2.01	2.56	1.58
	C:N = 151.5	ET	2.21	2.20	6.99	1.69	2.00
		U_N	0.04	0.04	0.04	0.04	0.04
		WUE	1.82	1.82	0.57	2.70	1.79
		NUE_{GPP}	100.50	**100.00**	100.25	114.00	89.50
		NUE_{NPP}	50.50	**50.00**	50.25	64.00	39.50
		L/C/W	4/8/0	**4/4/4**	4/8/0	6/6/0	7/5/0
Dry air	C = 7610	GPP	6.18	5.65	6.09	7.01	5.45
	N = 50.23	NPP	3.14	2.61	3.05	3.97	2.41
	C:N = 151.5	ET	3.41	3.07	10.59	2.60	3.05
		U_N	0.06	0.06	0.06	0.06	0.06
		WUE	1.81	1.84	0.58	2.70	1.79
		NUE_{GPP}	101.31	92.62	**99.84**	114.92	89.34
		NUE_{NPP}	51.48	42.79	**50.00**	65.08	39.51
		L/C/W	4/8/0	3/1/8	**4/4/4**	6/6/0	8/4/0
High CO_2	C = 8385	GPP	5.10	3.55	2.58	6.71	4.73
	N = 55.34	NPP	1.75	0.20	-0.77	3.36	1.38
	C:N = 151.5	ET	2.65	1.73	3.93	2.43	2.53
		U_N	0.07	0.07	0.07	0.07	0.07
		WUE	1.92	2.05	0.66	2.76	1.87
		NUE_{GPP}	76.12	52.99	38.51	**100.15**	70.60
		NUE_{NPP}	26.12	2.99	-11.49	**50.15**	20.60
		L/C/W	3/3/7	2/0/10	2/0/10	**4/4/4**	5/2/6
Low light	C = 7008	GPP	5.98	4.33	3.30	7.56	5.61
	N = 46.26	NPP	3.18	1.53	0.50	4.76	2.81
	C:N = 151.5	ET	3.19	2.15	5.12	2.77	3.05
		U_N	0.06	0.06	0.06	0.06	0.06
		WUE	1.87	2.01	0.64	2.73	1.84
		NUE_{GPP}	106.79	77.32	58.93	135.00	**100.18**
		NUE_{NPP}	56.79	27.32	8.93	85.00	**50.18**
		L/C/W	2/5/5	2/1/9	2/1/9	4/8/0	**4/4/4**

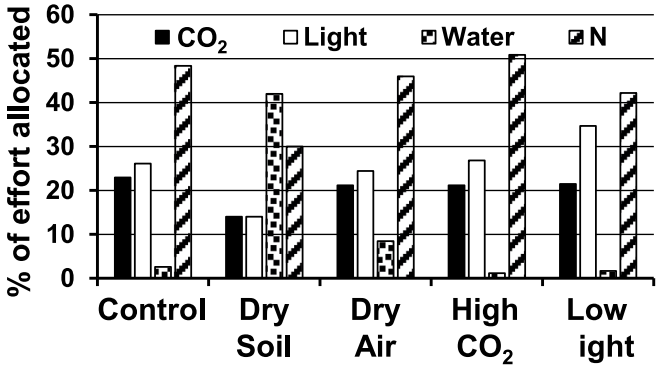

Fig. 9. Distribution of uptake effort among N and three interdependent resources, CO_2, light, and water. Vegetation acclimated to control, dry soil, dry air, high CO_2, and low light conditions. Effort allocated to N is simply the primary effort, V_N. Efforts allocated toward the interdependent resources are the primary C effort times the sub-effort allocated to each, V_C v_{CCa}, V_C v_{CI}, and V_C v_{CW}.

each by light, CO_2, and water (bold underlined font in cells along the main diagonal of Table 3). These results illustrate the ability of the model to maintain homeostasis based on resource optimization through effort allocation.

For simulations under conditions to which the vegetation is not acclimated, the nitrogen-use efficiency in most cases is either too high or too low to maintain stoichiometric balance. The cases where the stoichiometric balance is only slightly off are the vegetation acclimated to dry-soil and exposed to either control or dry-air conditions and the vegetation acclimated to dry-air exposed to control conditions, indicating that acclimation to water limitation is less disruptive of C-N stoichiometry than acclimation to low light or high CO_2.

In all cases the number of hours where photosynthesis is limited by light, CO_2, and water deviates from the balanced 4:4:4 (Table 3), indicating a wasteful pattern of effort allocation when the vegetation is not acclimated to the simulation conditions. For example, when the vegetation is acclimated to the control conditions and exposed to either dry soil or dry air, photosynthesis is only limited by light for three hours and to CO_2 for zero hours. Therefore, photosynthesis could be increased

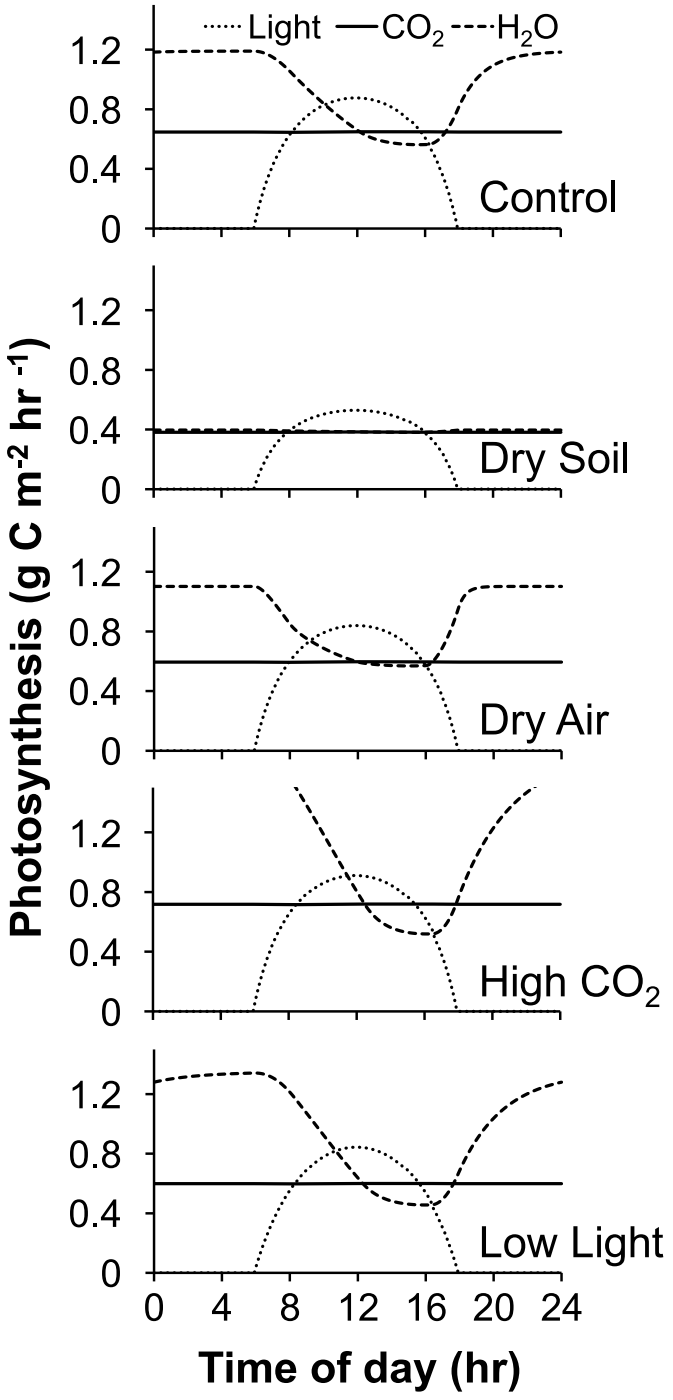

Fig. 10. Light-limited, CO_2-limited, and water-limited photosynthetic rates over 24-h simulations for vegetation acclimated to control, dry soil, dry air, high CO_2 and low light. The true photosynthetic rate is the minimum of these three rates.

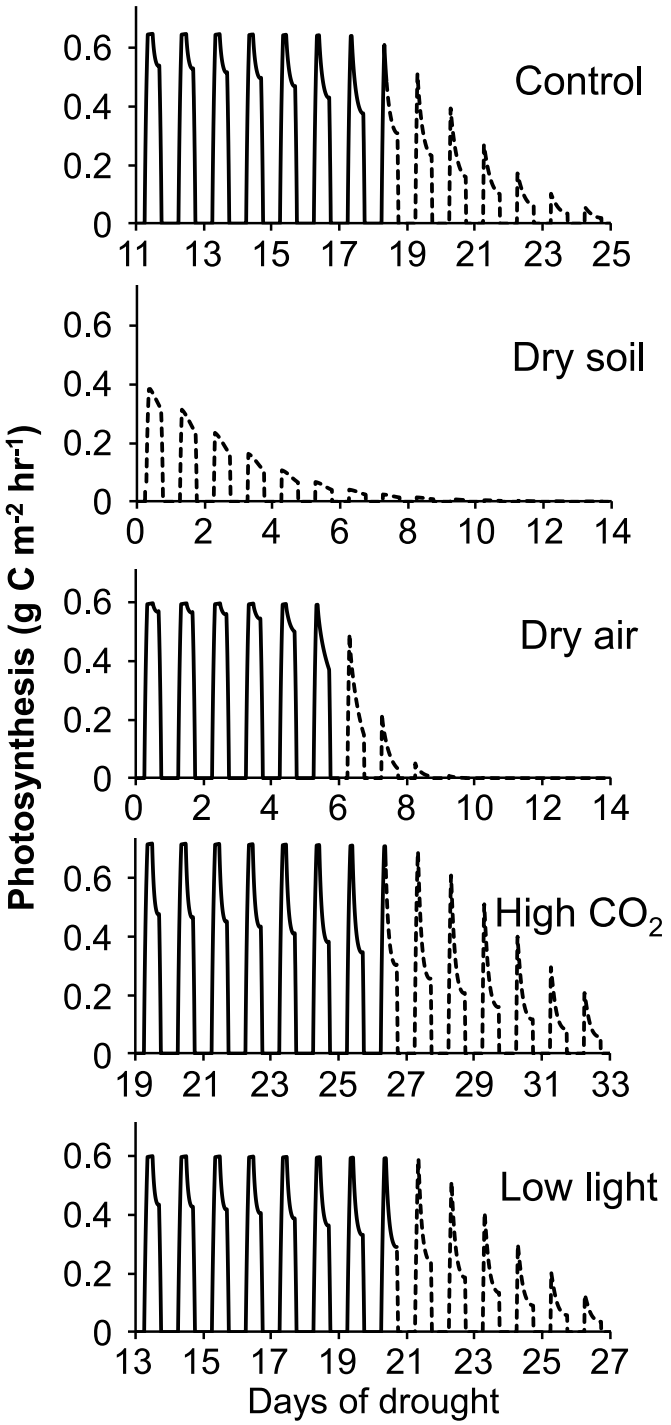

Fig. 11. Photosynthetic rates as vegetation acclimated to control, dry soil, dry air, high CO_2, and low light succumb to drought. All simulations were run under the conditions to which the vegetation was acclimated except that the soil water was not held constant. All simulations except the dry soil simulation start with soil water at field capacity (100 mm, -0.01 MPa); the dry soil simulation starts with soil water at about 40 mm soil water (-1 MPa). Dashed lines begin when soil water first drops below -1 MPa.

by reallocating effort away from light and CO_2 toward water. With the specified time constants on effort reallocation, the vegetation would not be expected to acclimate to the new conditions in such a short period of time. Over time, if the simulation conditions are maintained, the effort is reallocated to be less wasteful (as in Fig. 9 and the diagonal cells in Table 3).

Other metabolic indicators vary as would be expected across the conditions of the one-day simulations (rows in Table 3) but in more surprising ways across acclimation conditions (columns in Table 3). Because the manipulations are only of light, CO_2, and water, N uptake (U_N) is constant across simulation conditions (rows in Table 3) but varies in relation to the overall productivity under the acclimated conditions (columns in Table 3; highest acclimated to elevated CO_2, lowest acclimated to dry soils). For all acclimation conditions, simulations under the two most favorable conditions, elevated CO_2 and control, have the highest rates of photosynthesis (GPP) and net primary production (NPP). Transpiration is always highest in simulations with

dry air. Instantaneous water-use efficiency (U_C/T_R) is determined entirely by vapor pressure deficit and atmospheric CO_2 (Eq. 2.19) and therefore does not vary with biomass or effort allocation. The daily water-use efficiency (WUE = daily photosynthesis/ daily transpiration) therefore varies far less within the simulation conditions and across the acclimation conditions (columns in Table 3; CV < 7%) than within acclimation conditions and across simulation conditions (rows in Table3; CV > 36%).

Responses to drought following preadaptation to different interdependent light, CO_2, and water conditions: Finally, we run a set of simulations in which conditions are maintained the same as the acclimation conditions except we allow transpiration to dry the soil rather than holding the soil moisture constant (Fig. 11). Under dry soil conditions where the soil begins with a water potential of -1 MPa, photosynthesis declines immediately and effectively ceases within about 8 days. The afternoon depression in photosynthesis in this simulation is less steep than in the other simulations because of the high allocation to water acquisition and the consequent high hydraulic connectivity between soil and canopy. Under dry air conditions, there is a noticeable intensification of the afternoon depression in photosynthesis after four days, soils dry to -1 MPa by day 6, and photosynthesis effectively stops by day 10. Soil drying and photosynthetic decline are much more gradual in the other simulations with the time to reach -1 MPa of 18, 20, and 26 days in the control, low-light, and elevated-CO_2 simulations, respectively. In all three cases the high initial soil moisture and low vapor pressure deficit contributes to this long delay in photosynthetic collapse. With low light, the lower rate of photosynthesis also decreases transpiration (Eq. 2.19) and prolongs the delay before photosynthetic collapse. With elevated CO_2, the increase in water use efficiency prolongs the delay before photosynthetic collapse by another 6 days (Eq. 2.19). The photosynthetic collapse in these simulations is also more gradual than in the dry-air simulations, taking 8 to 10 days rather than just 5 days.

The dynamics in these simulations are dominated by the environmental conditions (especially initial soil water, vapor-pressure deficit) and the time course of the simulations is too short for reallocation of effort to have a significant effect. Nevertheless, the effects of resource optimization in the preadaptation to the five environmental conditions are important. In particular, the high allocation to water acquisition when preadapted to dry soil and dry air conditions helps accelerate the progression of drought. Conversely, the high water-use efficiency under elevated CO_2 and the low transpiration under low light decrease the allocation of effort toward water acquisition and thereby delay the onset of drought. These results are again consistent with what is expected under the resource optimization paradigm.

4. Conclusions

Organisms are continuously acclimating to a changing environment (Mooney 1972, Bloom et al. 1985, Chapin et al. 1987, Wikström and Ericsson 1995, Ågren and Bosatta 1996, Rastetter 2011). This acclimation has important ramifications for the distribution, storage, cycling, and throughput of elements in ecosystems. Here we build on the resource-optimization algorithm developed for the Multiple Element Limitation (MEL) model (Rastetter and Shaver 1992, Rastetter et al. 2013, Pearce et al. 2015, Nagy et al. 2017) by developing a hierarchical approach to simulating acclimation to changes in or requirements for substitutable and interdependent resources. The approach we use is based on an abstract quantity we call “effort” representing assets the organism has available to allocate toward resource acquisition. The effort is finite but can be reallocated among various resources. We first allocate effort among primary element resources (e.g., C, N, P) and then allocate that primary effort among substitutable sources of the primary resources (e.g., NH_4, or NO_3 as sources of N) or among resources that are interdepended toward the assimilation of a primary element resource (e.g., light, CO_2, and water to assimilate C through photosynthesis and associated transpiration). Allocation of effort among primary resources is based on maintaining the stoichiometric and metabolic balance of the organism. The approach for both substitutable and interdependent resources is to partition the primary effort by allocating sub-effort toward the resource with the highest marginal yield of the primary element resource per effort expended. The marginal yield is simply the incremental increase in element assimilation per incremental increase in effort expended, including effort expended to cover the cost of taking up and assimilating the resource.

Our algorithm for allocating effort among substitutable and interdependent resources produced results that are consistent with the predictions of the resource optimization paradigm, particularly as expressed in the economic analogue of Bloom et al. (1985) and Chapin et al. (1987). These results will, of course, need to be corroborated with data, but that corroboration is better done in the context of a more complex model. The current model provides a more heuristic perspective on resource optimization for substitutable and interdependent resources.

Our treatment of substitutable and interdependent resources is essentially the same. In both cases, we calculate a marginal yield of the element resource per incremental increase in effort expended and allocate effort away from resources with low margin yield and toward the resource with the highest marginal yield. The major difference between the two is that the organism can meet its requirements by taking up only one or a combination of several substitutable resources, but it must take up all interdependent resources concurrently. Because the organism can use any combination of substitutable resources, the major distinction among them is their relative acquisition and assimilation cost. The relative cost of interdependent resources is irrelevant because they are all essential regardless of cost. Thus, the cost needs to be factored into the calculation of marginal yield for substitutable resources (Eq. 1.24) but not for interdependent resources (Eq. 2.33). Also, because the sub-effort (v_{Nk}) allocated toward a substitutable resource can be zero if conditions do not favor its use, an initiator constant must be substituted into the allocation equation if the resource's use becomes favorable (ε_k in Eqs. 1.5 and 1.22). No such initiator is needed for interdependent resources because all interdependent resources are required concurrently and therefore sub-effort must always be allocated to them all.

Most multiple-resource limitation models simulate uptake potentials that increase with biomass but are otherwise prescribed and therefore do not acclimate to changes in the environment like the model we present here. Limitation in these models is typically based on Liebig's Law of the Minimum and thus a single resource limits growth; in our model acclimation drives uptake potentials toward a condition of equal limitation by all resources. The classic MacArthur and Levin (1964), Tilman (1982), and Droop (1973) models are good examples of this type of model, as are more recent models like Huisman and Weissing (2001), Rastetter and Ågren (2002), DeMalach et al. (2016), and Strauss et al. (2019). The DeMalach et al. (2016) model includes a resource-specific metabolic cost for resource acquisition like the one we use to distinguish among substitutable resources; this cost is used in the assessment of production but is not used to drive acclimation.

Other models handle multiple resource limitation with adaptive root-shoot ratios. Thornley (1972) modeled counter flows of C from shoot to root and N from root to shoot (a similar approach is used by Rastetter et al. 1991). Because both roots and shoots in the model are co-limited by C and N, the tissue responsible for acquiring the more limiting resource has first access to that resource, grows faster, consumes more of the limiting resource, and therefore starves the other tissue for the limiting resource. Thus, root-shoot ratios increase under N limitation and decrease under light limitation. Kooijman (2001) captures this root-shoot acclimation by simulating a “plant as a symbiosis between root and shoot.” Although our approach to multiple limitation is more abstract, we believe it is also more flexible and capable, for example, of addressing acclimation to changes in multiple soil resources or multiple canopy resources, as illustrated above.

In a series of papers, Dybzinski et al. (2011) and Farrior et al.

(2013a & b) used individual-based vegetation models like Tilman's (1988) ALLOCATE model to find the evolutionarily stable strategy for acquiring primary resources (light, nitrogen, and water). Within individual plants, uptake potentials for resources are fixed in these models except in the transition from understory to canopy individuals. The optimization is through variability among offspring and selection. Nevertheless, if applied in a dynamic setting, the selection of individuals as the environment changes would result in a vegetation level acclimation analogous to our model, but on a longer time scale. The Dybzinski-Farrior approach could readily be applied to substitutable and interdependent resources. Indeed, Good et al. (2018) apply a similar approach to substitutable resources.

The defining characteristic of the Anthropocene is the change to the global environment imposed by human activities. Mitigation, management, and adaptive strategies will require analysis and prediction of how ecosystems respond to this changing environment. Models designed for these purposes continue to improve. The approach to modeling we present here is general and should be applicable for addressing ecosystem responses to global change in a variety of settings. We believe the approach can be adapted to modeling efforts at local, regional, and global scales.

Author contributions

Rastetter: PI on grants supporting this research, code development, intellectual development of ideas, writing

Kwiatkowski: Development of computer code, intellectual development of ideas, writing and review of manuscript

Declaration of Competing Interest

This work was supported entirely by grants from the US National Science Foundation and no other entity other than the MBL and the NSF have any financial interest in the work. The authors declare that they have no known competing financial interests or personal relationships that could have appeared to influence the work reported in this paper.

Acknowledgments

This work was supported in part by the National Science Foundation under NSF grants 1651722, 1637459, 1603560, 1556772, 1841608. Any Opinions, findings and conclusions or recommendations expressed in this material are those of the authors and do not necessarily reflect those of the National Science Foundation.

References

Ågren, G., Bosatta, E., 1996. Theoretical Ecosystems Ecology; Understanding Element Cycles. Cambridge University Press, Cambridge, UK 234pp.
IIIBloom, A.J., Chapin, F.S., Mooney, H.A., 1985. Resource limitation in plants—an economic analogy. Ann. Rev. Syst. Ecol. 16, 363–392.
IIIChapin, F.S., Bloom, A.J., Field, C.B., Waring, R.H., 1987. Plant responses to multiple environmental factors. Bioscience 37, 49–57.
Clapp, R.B., Hornberger, G.M., 1978. Empirical equations for soil hydraulic properties. Water Resour. Res. 14, 601–604.
Cleveland, CC, Townsend, AR, Schimel, DS, Fisher, H, Howarth, RW, Hedin, LO, Perakis, SS, Latty, EF, von Fischer, JC, Elseroad, A, Wasson, MF, 1999. Global patterns of terrestrial biological nitrogen (N2) fixation in natural ecosystems. Global Biogeochem. Cycle. 13, 623–645.
Crews, TE., 1999. The presence of nitrogen fixing legumes in terrestrial communities: evolutionary vs ecological considerations. Biogeochemistry 46, 233–246.
DeMalach, N., Zaady, E., Weiner, J., Kadmon, R., 2016. Size asymmetry of resource competition and the structure of Plant communities. J. Ecol. 104, 899–910.
Droop, M.R., 1973. Some thoughts on nutrient limitation in algae. J. Phycol. 9, 264–272.
Dybzinski, R, Farrior, C., Wolf, A., Reich, P.B., Pacala, S.W., 2011. Evolutionarily stable strategy carbon allocation to foliage, wood, and fine roots in trees competing for light and nitrogen: an individual-based model and quantitative comparison to data. Am. Nat. 177, 153–166.
Farquhar, G.D., 1989. Models of integrated photosynthesis of cells and leaves. Phil. Trans. R. Soc. Lond. B 323, 357–367.
Farrar, J.F., Jones, D.L., 2000. The control of carbon acquisition by roots. New Phytol. 147, 43–53.
Farrior, C.E., Dybzinski, R., Levin, S.A., Pacala, S.W., 2013a. Competition for water and light in closed-canopy forests: a tractable model of carbon allocation with implications for carbon sinks. Am. Nat. 181, 314–330.
Farrior, C.E., Tilman, D., Dybzinski, R., Reich, P.B., Levin, S.A., Pacala, S.W., 2013b. Resource limitation in a competitive context determines complex plant responses to experimental resource additions. Ecology 94, 2505–2517.
Field, C., Chapin III, F.S., Matson, P.A., Mooney, H.A., 1992. Responses of terrestrial ecosystems to the changing atmosphere: a resource-based approach. Ann. Rev. Ecol. Syst. 23, 201–236.
Giese, AC., 1973. Cell Physiology, Fourth Ed. WB Saunders Company, Philadelphia, PA, USA.
Good, B.H., Martis, S., Hallatschek, O., 2018. Adaptation limits ecological diversification and promotes ecological tinkering during competition for substitutable resources. Proc. Nat Acacd. Sci. 115, E10407–E10416.
Gutschick, V.P., 1981. Evolved strategies in nitrogen acquisition by plants. Am. Nat. 118, 607–637.
Hilbert, D.W., 1990. Optimization of plant root:shoot ratios and internal nitrogen concentration. Ann. Bot. 66, 91–99.
Huisman, J., Weissing, F.J., 2001. Fundamental unpredictability in multispecies competition. Am. Nat. 157, 488–494.
Jiang, Y., EB Rastetter, E.B., Shaver, G.R., Rocha, A.V., Zhuang, Q., Kwiatkowski, B.L., 2017. Modeling long-term changes in tundra carbon balance following wildfire, climate change, and potential nutrient addition. Ecol. Appl. 27, 105–117. https://doi.org/10.1002/eap.1413.
Kooijman, S.A.L.M., 2001. Quantitative aspects of metabolic organization: a discussion of concepts. Phil. Trans. R. Soc Lond. B 356, 331–349.
Kröner, C., 2015. Paradigm shift in plant growth control. Curr. Opin. Plant Biol. 25, 107–114.
Lazarus 2.0.4 on http://www.lazarus-ide.org. 2019.
Leuning, R., 1995. A critical appraisal of a combined stomatal-photosynthesis model for C_3 plants. Plant. Cell Environ. 18, 339–355.
MacArthur, R., Levins, R., 1964. Competition, habitat selection, and character displacement in a patchy environment. Proc. Nat. Accad. Sci. US 51, 1207–1210.
Mooney, H.A., 1972. The carbon balance of plants. Ann. Rev. Ecol. Syst. 3, 315–346.
Nagy, R.C., Rastetter, E., Neill, C., Porder, S., 2017. Nutrient limitation in tropical secondary forests following different management practices. Ecol. Appl. 27, 734–755.
Olson Jr., R.L., Sharpe, P.J.H., Wu, H.-I., 1985. Whole-plant modeling: a continuous-time Markov (CTM) approach. Ecol. Model. 29, 171–187.
Parton, W.J., Scurlock, J.M.O., Ojima, D.S., Gilmanov, T.G., Scholes, R.J., Schimel, D.S., Kirchner, T., Menaut, J.-C., Seastedt, T., Garcia Moya, E., Kamnalrut, A., Kinyamario, J.I., 1993. Observations and modeling of biomass and soil organic matter dynamics for the grassland biome worldwide. Global Biogeochem. Cycle. 7, 785–809.
Pearce, A.R., Rastetter, E.B., Bowden, W.B., Mack, M.C., Jiang, Y., Kwiatkowski, B.L., 2015. Recovery of arctic tundra from thermal erosion disturbance is constrained by nutrient accumulation: a modeling analysis. Ecol. Appl. 25, 1271–1289.
Press, W.H., Flannery, B..P, Teukolsky, S.A., Vetterling, W.T., 1986. Numerical Recipes: The Art of Scientific Computing. Cambridge University Press, Cambridge, UK.
Rastetter, E.B., 2011. Modeling coupled biogeochemical cycles. Front. Ecol. Environ. 9, 68–73.
Rastetter, E.B., 2017. Modeling for understanding v. modeling for numbers. Ecosystems 20, 215–221.
Rastetter, E.B., Ågren, G.I., 2002. Changes in individual allometry can lead to species coexistence without Niche separation. Ecosystems 5, 789–801.
Rastetter, E.B., Ågren, G.I., Shaver, G.R., 1997. Responses of N-limited ecosystems to increased CO2: A balanced-nutrition, coupled-element-cycles model. Ecol. Appl. 7, 444–460.
Rastetter, E.B., King, A.W., Cosby, B.J., Hornberger, G.M., O'Neill, R.V., Hobbie, J.E., 1992. Aggregating fine-scale ecological knowledge to model coarser-scale attributes of ecosystems. Ecol. Appl. 2, 55–70.
Rastetter, E.B., Ryan, M.G., Shaver, G.R., Melillo, J.M., Nadelhoffer, K.J., Hobbie, J.E., Aber, J.D., 1991. A general biogeochemical model describing the responses of the C and N cycles in terrestrial ecosystems to changes in CO2, climate and N deposition. Tree Physiol. 9, 101–126.
Rastetter, E.B., Shaver, G.R., 1992. A model of multiple element limitation for acclimating vegetation. Ecology 73, 1157–1174.
Rastetter, E.B., Vitousek, P.M., Field, C., Shaver, G.R., Herbert, D., Ågren, G.I., 2001. Resource optimization and symbiotic N fixation. Ecosystems 4, 369–388.
Rastetter, E.B., Yanai, R.D., Thomas, R.Q., Vadeboncoeur, M.A., Fahey, T.J., Fisk, M.C., Kwiatkowski, B.L., Hamburg, S.P., 2013. Recovery from disturbance requires resynchronization of ecosystem nutrient cycles. Ecol. Appl. 23, 621–642.
Ryan, M.G., Hunt, E.R., Jr., McMurtrie, R.E., Ågren, G.I., Aber, J.D., Friend, A.D., Rastetter, E.B., Pulliam, W., Raison, J., Lindner, S., 1996. Comparing models of ecosystem function for temperate conifer forests. I. Model description and validation. Breymeyer, A., Hall, D.O., Melillo, J.M., Ågren, G.I. (Eds.), Comparing models of ecosystem function for temperate conifer forests. I. Model description and validation. Global Change: Effects on Coniferous Forests and Grasslands 313–362 SCOPE 56.
Shaver, G.R., Melillo, J.M., 1984. Nutrient budgets of marsh plants: efficiency concepts and relation to availability. Ecology 65, 1491–1510.
Strauss, A.T., Shoemaker, L.G., Seabloom, E.W., Borer, E.T., 2019. Cross-scale dynamics in community and disease ecology: relative timescales shape the community ecology of pathogens. Ecology 00 (00), e02836. https://doi.org/10.1002/ecy.2836. 10.1002/ecy.2836.
Thornley, J.H.M., 1972. A balanced quantitative model for root:shoot ratios in vegetative plants. Ann. Bot.-Lond. 36, 431–441.
Tilman, D., 1982. Resource Competition and Community Structure. Monographs in

Population Biology 17 Princeton University Press 296pp.
Tilman, D., 1988. Plant Strategies and the Dynamics and Structure of Plant Communities. Princeto University Press, Princeton, NJ, USA 360 pp.
Vallino, J.J., Hopkinson, C.S., Hobbie, J.E., 1996. Modeling bacterial utilization of dissolved organic matter: optimization replaces Monod growth kinetics. Limnol. Oceanogr. 41, 1591–1609.
Wikström, F., Ericsson, T., 1995. Allocation of mass in trees subject to nitrogen and magnesium limitation. Tree Phys. 15, 339–344.
Williams, M., Rastetter, E.B., Fernandes, D.N., Goulden, M.L., Wofsy, S.C., Shaver, G.R., Melillo, J.M., Munger, J.M., Fan, S.-M., Nadelhoffer, K.J., 1996. Modelling the soil-plant-atmosphere continuum in a *Quercus-Acer* stand at Harvard Forest: the regulation of stomatal conductance by light, nitrogen and soil/plant hydraulic properties. Plant Cell Environ. 19, 911–927.